# Delay-induced spatial correlations in one-dimensional stochastic networks with nearest-neighbor coupling

Andrey Pototsky and Natalia B. Janson
*Department of Mathematical Sciences, Loughborough University, Loughborough, Leicestershire LE11 3TU, United Kingdom*
(Received 8 September 2009; published 8 December 2009)

We consider a network of deterministic and stochastic locally coupled oscillators with positive or negative dissipation and local time-delayed feedback. (i) For a deterministic system, we study propagation of waves through the network. We show that time delay leads to a coexistence of several neutral modes with different wave numbers and group velocities, which we compute analytically. (ii) For noisy system, we study the response of the network to external random forcing correlated in space and uncorrelated in time. Below the threshold of spatial instability, noise induces spatiotemporal fluctuations, which can be characterized by the structure function. We give an analytical expression for the structure function and demonstrate the effect of the time delay and of the correlation length of noise on the wave number of the most excited mode.

DOI: 10.1103/PhysRevE.80.066203 PACS number(s): 89.75.Kd, 02.30.Ks, 05.40.Ca, 46.40.−f

## I. INTRODUCTION

Periodic structures consisting of a large number of elastic or stiff identical beams or plates coupled to adjacent neighbors find various important applications in engineering. Stiff beams on elastic supports serve as a basis for high-storey buildings. Elastic plates on regularly spaced stiffeners are typical in the aeroplane design, where they are used to construct fuselage structure or a wing. Understanding of vibrational properties of these periodic structures in response to deterministic or random forcing is crucial as it provides us with information about critical loads and forces, which may lead to breakdown of the whole structure.

From the theoretical viewpoint the propagation of waves in linear [1–6] and nonlinear [7–9] periodically supported beam has been intensively studied in the past. It has been shown that in the damping-free case [1,2], i.e., in the case when every single beam oscillates without damping, harmonic waves can propagate in the system provided that their frequencies lie within the so-called "propagation zones." The waves with other frequencies die out with fixed decay rate as they spread. For a nonzero damping, free waves can no longer exist without external forcing [3,8]. Due to omnipresence of fluctuations and noise in real life the random external forcing can never be eliminated. Depending on the statistical properties of the fluctuating external field, different modes are being constantly excited in the system with different energies (amplitudes). Response of a periodically supported beam to convected random loading and to forcing by random acoustic wave has been studied in [10,11], where the average amplitude of the beam curvature was determined.

In spatially extended systems, time delays appear naturally due to the finite propagation times of the perturbations. The role of global and local time delay feedback in spatially extended systems has been extensively studied. From the viewpoint of spatiotemporal pattern formation, time delay can modify, suppress, or even induce spatial instability [12–18]. Below the stability threshold, i.e., when the homogeneous steady state is stable, external noise leads to permanent excitation of stable modes and, therefore, serves as indicator for instability. This effect is known as noisy precursor of bifurcations [19,20]. The response of a spatially discrete periodic system to random fluctuations can be characterized by the space-correlation function $G(i)$, which is computed as ensemble averaged product of the displacements $x_i(t)$ of the $i$th element, i.e., $G(i)=\lim_{N\to\infty}(1/N)\Sigma_{j=1,N}x_j(t)x_{j+i}(t)$, where $N$ denotes the number of elements in the periodic chain. Spatially Fourier-transformed correlation function $S(k)=\Sigma_{(j=0,N-1)}G(j)\exp(2\pi Ikj/N)$, where $I=\sqrt{-1}$, is called structure function [20]. In what follows, we will refer to the critical values of system parameters at which the homogeneous steady state loses its stability as a stability threshold. With this, "below the threshold" denotes a stable homogeneous steady state. Close to stability threshold, the structure function attains maximum at a certain wave number $k_{\max}$ which is close to the wave number $k_{\mathrm{LS}}$ of the least stable mode in the spatially periodic system. Further away from the stability threshold, the dominance of the mode $k_{\mathrm{LS}}$ becomes less pronounced, which leads to the increased difference between the two wave numbers $k_{\max}$ and $k_{\mathrm{LS}}$.

Apart from the applications in engineering, a chain of locally coupled oscillators can be used to study the phenomenon of synchronization which is relevant to some physical and biological systems such as neural networks. An extensive overview of neural dynamics and of signal transmissions through a network can be found, for instance, in Ref. [21]. The effects of noise and of time delays on the stability of phase-locked states in neural networks have been addressed in Refs. [22,23]. Exponential stability of networks with delay and deterministic input signals was considered in Refs. [24–26]. However, it should be emphasized that in case of neural networks, a single element (oscillator) is assumed to be in the excitable regime, when decoupled from the rest of the system. This makes the problem essentially nonlinear.

Here, motivated by various applications in engineering [2,4] and physics [27], we focus on a chain of linear damped oscillators with time-delayed feedback coupled locally via a diffusive coupling to a random forcing correlated in space and uncorrelated in time.

The main results are as follows:

(i) First, we study the propagation of wave packets through the network. We show that finite delay times induce

 

multiplicity of neutral modes, which correspond to a zero attenuation coefficient. We analytically compute the wave number as well as the group velocity of neutral modes as a function of the delay time.

(ii) Second, we give an analytical expression for the structure function of the system driven by additive space-correlated noise.

(iii) Third, we show that noisy precursor of the delay-induced spatial instability is strongly affected by the correlation length of the external fluctuating field. In other words, for a fixed subcriticality, there exists a finite correlation length of noise for which the maximum in the structure function disappears and the bifurcation can no longer be detected.

## II. MODEL: RING OF LOCALLY COUPLED NOISY DAMPED OSCILLATORS WITH TIME-DELAYED FEEDBACK

We consider a ring of $N$ damped oscillators with time delay coupled locally via a diffusive coupling. The evolution equations for the $i$th oscillator are given by

$$\ddot{x}_i = \varepsilon \dot{x}_i - \omega_0^2 x_i + K(\dot{x}_i^{(\tau)} - \dot{x}_i) + \sigma(x_{i+1} + x_{i-1} - 2x_i) + \sqrt{2D}\xi_i(t), \tag{1}$$

where $\tau$ is the delay time, $\dot{x}_i^{(\tau)} = \dot{x}_i(t-\tau)$, $\sigma$ is a strength of the local coupling, $D$ is the noise intensity, and $\xi_i(t)$ has the space-time correlation function given by $\langle \xi_i(t)\xi_k(t')\rangle = \alpha \exp(-\alpha|i-k|)\delta(t-t')$. The discrete spatial Fourier transform of $\alpha \exp(-\alpha|i-k|)$ is obtained as $\hat{g}(\tilde{\omega}) = \alpha^2/(\alpha^2+\tilde{\omega}^2)$, with $\tilde{\omega}^2$ given by $2[1-\cos(\frac{2\pi k}{N})]$ [20]. The discrete wave number $k$ changes in the limits from $k=0$ to $N-1$.

The particular choice of the form of the delayed feedback is to some extent arbitrary and was taken as one of the simplest possible, also following the earlier works on the control of noise-induced oscillations for consistency [28,29]. However, the same approach can be used to obtain analytical results for other forms of linear delayed feedback.

## III. ANALYSIS OF THE NOISE-FREE SYSTEM

### A. Stability

Before studying the subthreshold noise-induced fluctuations in Eq. (1), we need to determine the stability domain in the deterministic case, i.e., in the case of $D=0$. The noise-free Eq. (1) has a trivial homogeneous stationary solution $x_i = \dot{x}_i = 0$. Introducing new variable $y_i = \dot{x}_i$ we can rewrite Eq. (1) as a set of $2N$ first-order equations. Taking discrete spatial Fourier transform of $N$-dimensional vectors $x_i$, $y_i$, and $\xi_i$, we obtain in the Fourier space

$$\dot{\hat{x}}_k = \hat{y}_k,$$

$$\dot{\hat{y}}_k = \varepsilon \hat{y}_k - \omega_0^2 \hat{x}_k + K[\hat{y}_k(t-\tau) - \hat{y}_k] + \hat{x}_k 2\sigma\left[\cos\left(\frac{2\pi k}{N}\right) - 1\right], \tag{2}$$

where $\hat{x}_k$ and $\hat{y}_k$ denote the $k$th Fourier component of $x_i$ and $y_i$, respectively. Note that in the Fourier space, the equations in Eq. (2) are decoupled. This holds only for a chain of uniform oscillators driven by additive noise, i.e., for the noise intensity $D$, which does not depend on the variables $(x_i, y_i)$.

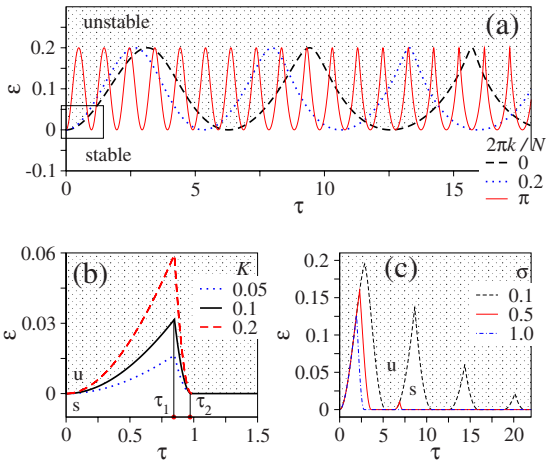


FIG. 1. (Color online) (a) Loci of the Andronov-Hopf bifurcation of the trivial state $x_i = y_i = 0$ in the parameter plane $(\tau, \varepsilon)$ for $\sigma = 10$ and $K = 0.1$. Solid, dashed, and dotted lines correspond to different values of the wave number $2\pi k/N$ as in the legend. A given wave number is stable below the corresponding line and is unstable above it. (b) Stability threshold of the trivial state for different $K$. On the solid line for $\tau \in [0, \tau_1]$ the trivial state becomes unstable via a Andronov-Hopf bifurcation of the homogeneous mode $k=0$; for $\tau \in [\tau_1, \tau_2]$ the shortest possible mode with $k=N/2$ loses its stability. For $\tau_2 < \tau < \tau_3$ there exists only one neutral mode with a finite wave number $0 < 2\pi k/N < \pi$. For $\tau > \tau_3$ several modes become unstable simultaneously. Critical delay times $\tau_2$ and $\tau_3$ are given by $\tau_2 = 2\pi/\sqrt{\omega_0^2 + 4\sigma}$ and by $\tau_3 = 2\tau_2$. (c) Same as in (b) for different values of $\sigma$ as given in the legend.

Stability threshold is determined from the Jacobi matrix of Eq. (2) by setting the real part Re $\lambda$ of the eigenvalue $\lambda$ to zero. Trivial stationary state $x_i = y_i = 0$ becomes unstable either via Andronov-Hopf bifurcation at $k=0$ or via an oscillatory Turing bifurcation at $k \neq 0$. Critical values of the parameters are found from the following set of equations:

$$0 = -\Omega^2 - \Omega K \sin \Omega\tau + \omega^2, \quad 0 = \varepsilon - K + K \cos \Omega\tau, \tag{3}$$

where $\Omega$ is the imaginary part of the eigenvalue $\lambda$ and $\omega^2 = \omega_0^2 - 2\sigma[\cos(2\pi k/N) - 1]$.

In the uncoupled case, i.e., for $\sigma = 0$ the stability threshold in the parameter space $(\varepsilon, \tau)$ is shown in Fig. 1(a) by a dashed line. The trivial state is stable in the region below this line and unstable in the area above it (shaded region). Note that the stability threshold for the homogeneous mode $k=0$ is given by the same line as for $\sigma = 0$ and $K = 0.1$. To avoid confusion we will refer throughout the paper to the mode with $k=0$ as to the *homogeneous mode*, contrary to the *neutral mode*, which stands for the mode with zero real part of its eigenvalue.

For $\sigma \neq 0$, the stationary solution is stable if Re $\lambda < 0$ for all $N/2$ modes. It should be emphasized that the shortest possible wavelength has a spatial period equal to 2 which

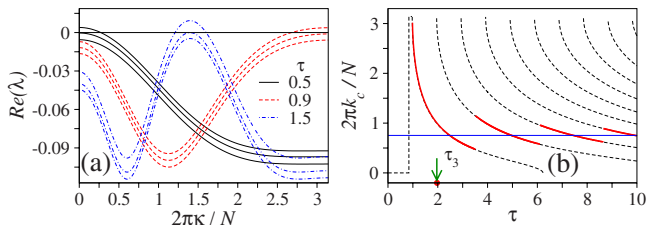


FIG. 2. (Color online) (a) Dispersion relation: real part of the largest eigenvalue λ vs wave number $2\pi k/N$ for $\sigma=10$, $K=0.1$, and three different values of the delay time $\tau$ as in the legend. For each $\tau$ the real part Re λ is plotted for three different $\varepsilon$: slightly below the corresponding critical value, directly at the threshold, and slightly above the critical value. (b) Critical wave number $2\pi k_c/N$ of the neutral mode for $\varepsilon=0$, as a function of $\tau$, as computed from Eq. (4). For $\tau>\tau_3$ there exist several neutral modes. Thick solid lines indicate the wave number of the neutral mode with the highest group velocity. Solid horizontal line represents the limiting value of the wave number of the fastest neutral mode.

corresponds to the wave number $2\pi N/(2N)=\pi$. As the wave number $2\pi k/N$ increases, the stability threshold which corresponds to this particular $2\pi k/N$ changes as illustrated in Fig. 1(a): dotted and solid lines show stability thresholds for $2\pi k/N=0.2$ and $2\pi k/N=\pi$, respectively, for $\sigma=10$. As we see, almost for all values of the delay time $\tau$, the trivial state becomes unstable at $\varepsilon=0$ except for the small area around the origin which is marked by a box in Fig. 1(a). In this area the lines correspond to the shortest possible wavelength equal to 2 (with $k=N/2$) and to the homogeneous mode $k=0$, which form the boundary of the stability domain. The enlarged area around the origin together with the stability threshold of the trivial state is shown in Fig. 1(b). The solid line corresponds to $\sigma=10$ and $K=0.1$. Dashed and dotted lines in Fig. 1(b) show how the stability threshold changes with the feedback strength $K$ which values are given in the legend.

The number of lobes of stability in the parameter plane $(\varepsilon,\tau)$ becomes bigger if $\sigma$ decreases. This is demonstrated in Fig. 1(c). As we see, for $\sigma=0.1$ there are four lobes of stability, while for a larger coupling ($\sigma=0.5$) only two lobes remain.

Different scenarios of spatial instability are demonstrated in Fig. 2(a), where the real part of the largest eigenvalue Re λ is shown as a function of the wave number $2\pi k/N$ for the same parameters as for the solid line in Fig. 1(b). There are three critical values of the delay time $\tau$ denoted by $\tau_1$, $\tau_2$, and $\tau_3$ at which the bifurcation scenario changes qualitatively. Thus, $\tau_1$ is defined as a double Hopf point. At this point two modes become unstable simultaneously: the homogeneous mode with $k=0$ and the shortest possible mode with $2\pi k/N=\pi$. For $\tau_1<\tau<\tau_2$, the shortest possible mode becomes unstable. The value of $\tau_2$ can be computed analytically from Eq. (3), $\tau_2=2\pi/\sqrt{\omega_0^2+4\sigma}$. For $\tau_2<\tau<\tau_3$, only one mode becomes unstable with a finite value of the wave number $0<2\pi k/N<\pi$. For $\tau>\tau_3$ several modes lose their stability simultaneously. Note that $\tau_3$ is related to $\tau_2$ as $\tau_3=2\tau_2=4\pi/\sqrt{\omega_0^2+4\sigma}$.

When crossing the threshold on the left branch, i.e., when $\tau\in[0,\tau_1]$ in Fig. 1(b), the trivial state loses its stability via Andronov-Hopf bifurcation with the wave number $k=0$. The corresponding bifurcation scenario is shown in Fig. 2(a) by solid lines. On the right branch, $\tau\in[\tau_1,\tau_2]$, the trivial state becomes unstable via an oscillatory Turing bifurcation with the wavelength 2; wave number equals $2\pi k/N=\pi$. The corresponding bifurcation scenario is shown by dashed lines in Fig. 2(a). Bifurcation scenario for $\tau_2<\tau<\tau_3$ is demonstrated by dashed-dotted lines in Fig. 2(a). For simplicity, the case when several modes lose their stability simultaneously is not shown.

For $\varepsilon=0$ the critical wave number $2\pi k_c/N$, which corresponds to the neutral mode with $\mathrm{Re}(\lambda)=0$, can be computed analytically from Eq. (3). It is given by

$$\frac{2\pi k_c}{N}=\arccos\left[\frac{\omega_0^2+2\sigma-\left(\frac{2\pi m}{\tau}\right)^2}{2\sigma}\right], \tag{4}$$

where index $m$ numbers the critical modes, i.e., ($m=1,2,\ldots$).

Figure 2(b) shows $2\pi k_c/N$ directly on the stability threshold, i.e., for $\varepsilon=0$, as a function of the delay time $\tau$ for the parameters as for the solid line in Fig. 1(b). Several modes become unstable simultaneously for $\tau>\tau_3$.

### B. Group velocity of neutral modes in the noise-free system

We now study the propagation of neutral modes, which correspond to a vanishing real part of the leading eigenvalue. As pointed out in the previous section [see Fig. 1(b)], the stability threshold is given by $\varepsilon=0$ for $\tau>\tau_2$. In this case the system becomes unstable via an oscillatory Turing instability with, in general, multiple neutral modes with the corresponding critical wave numbers $2\pi k_c/N$ given by Eq. (4). For $\tau_1<\tau<\tau_2$, the critical $\varepsilon$ is positive and the neutral mode has the wave number $2\pi k_c/N=\pi$. For $0<\tau<\tau_1$, the only neutral mode is the homogeneous one with $2\pi k_c/N=0$.

Every neutral mode with a specific wave number $2\pi k_c/N$ gives rise to a propagating wave packet, in which group velocity $V_G$ is given by the derivative $V_G=\partial\Omega(2\pi k/N)/\partial(2\pi k/N)$, computed at the corresponding critical wave number $2\pi k/N=2\pi k_c/N$. Multiplicity of neutral modes leads to the fact that several wave packets with different wave numbers can propagate through the system simultaneously.

To compute the group velocity of neutral modes, we notice that for the critical wave number $2\pi k_c/N$, the derivative of the real part Re(λ) of any neutral mode vanishes; i.e., we have two additional conditions on λ: $\mathrm{Re}(\lambda)=0$ and $\partial\,\mathrm{Re}(\lambda)(2\pi k/N)/\partial(2\pi k/N)=0$ at $2\pi k/N=2\pi k_c/N$. Now, by setting $\varepsilon=0$ and by differentiating the first equation in Eq. (3) with respect to $2\pi k/N$, we obtain

$$(V_G)_m=\frac{\tau\left\{4\sigma^2-\left[\omega_0^2+2\sigma-\left(\frac{2\pi m}{\tau}\right)^2\right]^2\right\}^{0.5}}{2\pi m(2+K\tau)}, \tag{5}$$

where index $m$ numbers the neutral modes as in Eq. (4).

It is worthwhile pointing out that Eq. (5) works only for $\tau>\tau_2$. For $\tau<\tau_2$, the neutral mode has the wave number

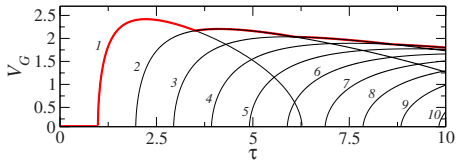


FIG. 3. (Color online) (a) Group velocity $V_G$ of neutral modes as a function of $\tau$ as computed from Eq. (5) for $\varepsilon=10$ and $K=0.1$. Numbers indicate the index of the neutral mode; thick solid line highlights the largest group velocity.

either equal to zero (homogeneous mode) or to $2\pi k_c/N=\pi$ (shortest possible mode). By differentiating the second equation in Eq. (3) with respect to $2\pi k/N$, one can show that the group velocity of these two modes is zero.

In Fig. 3 we show $V_G$ as a function of $\tau$ for $\sigma=10$ and $K=0.1$. Numbers near each curve indicate the mode index $m$ and the thick solid line highlights the largest values of $V_G$. The wave numbers $2\pi k_c/N$ of all neutral modes are shown in Fig. 2(b) by dashed lines. The wave number of the fastest neutral mode depends piecewise continuously on $\tau$, as indicated by the thick solid line in Fig. 2(b). For small $\tau$, the wave number of the fastest mode gradually decreases, but as $\tau$ becomes very large, the index $m_f$ of the fastest mode grows with $\tau$ linearly according to

$$m_f = \frac{\tau}{2\pi}(\omega_0^2 + 4\sigma)^{1/4}. \tag{6}$$

This leads to a saturation of the wave number of the fastest neutral mode, i.e.,

$$\lim_{\tau\to\infty}\frac{2\pi k_c}{N} = \arccos\left[\frac{\omega_0^2 + 2\sigma - \sqrt{(\omega_0^2+4\sigma)}}{2\sigma}\right]. \tag{7}$$

For $\sigma=10$, the limiting values of $\lim_{\tau\to\infty}\frac{2\pi k_c}{N}=0.7527$, as shown in Fig. 2(b) by a horizontal line.

To illustrate the possibility of propagation of wave packets with multiple wave numbers, we solve Eq. (1) numerically for $N=2048$, $\sigma=10$, $K=0.1$, and fixed delay time $\tau=5$. To set up a wave packet with a specific wave number $2\pi k_c/N$, we use the following initial conditions: the initial profile $x_i(t=0)=\exp[-g(i-1024)^2]\cos(2\pi i k_c/N)$ and initial velocities $\dot{x}_i=y_i(t=0)=0$, where $g$ represents the initial width of the wave packet.

Time evolution of the first neutral mode, i.e., $m=1$, is shown in Figs. 4(a)–4(c). Two wave packets with identical wave numbers propagate in opposite directions with the group velocity $V_G$. The width of each packet increases and its amplitude decreases with time due to dispersion and attenuation of other stable modes, which form the packet. The evolution of the second $m=2$, slightly shorter mode, is shown in Figs. 4(d)–4(f) at the same time moments as in Figs. 4(a)–4(c). Group velocity is visualized by computing the position of the amplitude of the packet as a function of time. Figure 4(g) represents the comparison between the time evolution of the maximum of $x_i$ computed numerically (dashed lines) and motion with the group velocity $i_{\max}=1024-V_G t$, with $V_G$, computed analytically from Eq. (5).

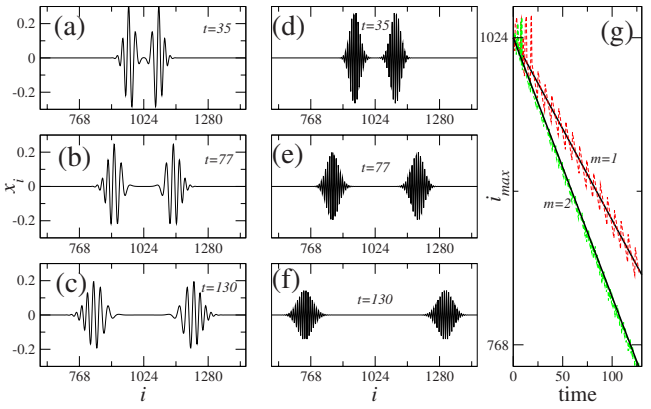


FIG. 4. (Color online) [(a)–(c)] Snapshots of the wave packet with the wave number $2\pi k_c/N$, which corresponds to the first mode, i.e., $m=1$. Parameters are $\varepsilon=0$, $\sigma=10$, $K=0.1$, and $\tau=5$. Time is indicated by numbers in each panel. [(d)–(f)] Same as in (a)–(c) but for the second neutral mode with $m=2$. (g) Time evolution of the position of the maximum of $x_i$: dashed lines—numerical simulations; solid lines—motion with the group velocity $i_{\max}=1024-V_G t$, where $V_G$ is given by Eq. (5).

To conclude this section, we have shown the twofold action of time delay on the propagation of waves through the system of coupled oscillators. First, time delay leads to the existence of multiple neutral modes. Second, by changing $\tau$, we can change the wave number of the neutral modes together with their group velocity.

### C. Subthreshold noise-induced fluctuations

Below the stability threshold, additive noise induces fluctuations in system equation (1). This fluctuations can be characterized by the space-correlation function $G(i)$, given by $G(i)=\langle x_j(t)x_{j+i}(t)\rangle$, where $\langle\ldots\rangle$ denotes ensemble average. According to the Wiener-Khinchin theorem, the discrete spatial Fourier transform $S(k)=\Sigma_{j=1,N}G(j)\exp(2\pi Ijk/N)$ of the function $G(i)$ is given by

$$S(k) = \langle\hat{x}_k(t)\hat{x}_k(t)\rangle = \Phi_{x_k}(0), \tag{8}$$

where $\Phi_{x_k}(\zeta)$ is the time-correlation function of $\hat{x}_k$, which is the Fourier transform of $x_i$. Note that the function $S(k)$ is also known as structure function [20]. Physical meaning of the structure function is the energy of fluctuations with the wave number $2\pi k/N$.

As pointed out in the introduction, in stable systems close to their stability threshold noise can serve as an indicator for instability or bifurcation. This effect is known as noisy precursor of bifurcations [19,20]. In zero-dimensional systems close to the point of bifurcation, the power spectrum of noise-induced fluctuations has a characteristic maximum near the onset frequency of the bifurcation. Similarly, in spatially extended systems, the structure function attains a maximum close to the critical wave number.

To compute the structure function $S(k)$, we consider noisy equation (1). Taking the discrete spatial Fourier transform, we notice that the correlation function of the Fourier-transformed noise $\eta_k(t)=\Sigma_{(i=0,N-1)}\xi_i(t)\exp(2\pi ikI/N)$ is given

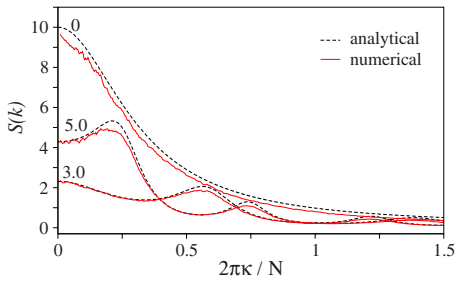


FIG. 5. (Color online) Structure function $S$ in units of the noise intensity $DN$ as a function of the wave number $2\pi k/N$ for $\alpha=\infty$, $\varepsilon=-0.05$, $\sigma=10$, $K=0.1$, and different $\tau$ as given by a number near each line. Solid lines correspond to $S$ computed numerically for a ring of $N=2048$ coupled oscillators; dashed lines obtained from the analytic expression Eq. (10).

by $\langle \eta_i(t)\eta_k(t')\rangle = \hat{g}(k)\delta_{ik}N\delta(t-t')$, where $\delta(x)$ is the Dirac delta function and $\delta_{ik}$ is Kronecker delta. This yields

$$\dot{\hat{x}}_k = \hat{y}_k,$$

$$\dot{\hat{y}}_k = \varepsilon\hat{y}_k - \omega^2\hat{x}_k + K[\hat{y}_k(t-\tau) - \hat{y}_k] + \sqrt{2D\hat{g}(k)N}\hat{\xi}_k(t), \quad (9)$$

where, as before, $\omega^2=\omega_0^2-2\sigma[\cos(\frac{2\pi k}{N})-1]$, $\hat{g}(k)=\alpha^2/\{\alpha^2-2[\cos(\frac{2\pi k}{N})-1]\}$, and $\hat{\xi}_k(t)$ are independent Gaussian variables with the correlation function $\langle\hat{\xi}_i(t)\hat{\xi}_k(t')\rangle=\delta_{ik}\delta(t-t')$.

Time-correlation function $\Phi_{x_k}(\zeta)$ of Eq. (9) was found analytically for negative $\varepsilon$ in Refs. [28,29]. According to Ref. [28], the closed analytic expression for the variance $\langle x_k^2\rangle$ is given in units of the noise intensity $DN$ by

$$\frac{\langle x_k^2\rangle}{DN} = \frac{\Phi_{x_k}(0)}{DN} = \hat{g}(k)\left[\frac{E}{R} + Fe^{\gamma\tau}\left(\frac{E}{R}\cos W\tau + \frac{1}{R}\sin W\tau\right)\right], \quad (10)$$

where

$$W = \sqrt{\omega^2 - \frac{(\varepsilon-K)^2-K^2}{4}}, \quad \gamma = \frac{\sqrt{(\varepsilon-K)^2-K^2}}{2},$$

$$F = -\frac{\varepsilon-K}{K} - \frac{\sqrt{(\varepsilon-K)^2-K^2}}{K},$$

$$E = \frac{W + Fe^{(-\gamma\tau)}(\gamma\sin W\tau - W\cos W\tau)}{\gamma - Fe^{(-\gamma\tau)}(\gamma\cos W\tau + W\sin W\tau)},$$

$$R = [K + F(\varepsilon-K)]e^{(-\gamma\tau)}[(\gamma^2-W^2)(E\cos W\tau + \sin W\tau) + 2W\gamma(E\sin W\tau - \cos W\tau)] + [(\gamma^2-W^2)E - 2\gamma W] \times(\varepsilon - K + KF). \quad (11)$$

Note that in the limit of the uncorrelated noise, i.e., for $\alpha\to\infty$, the wave number $2\pi k/N$ enters Eq. (10) solely through the function $W$.

In case of the uncorrelated noise ($\alpha=\infty$), the structure function $S/DN$ is shown for fixed $\sigma=10$ in Fig. 5 for three different delay times, as indicated by numbers near each line.

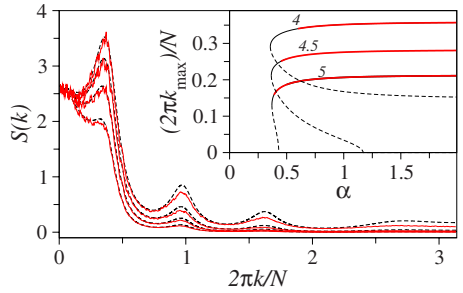


FIG. 6. (Color online) Structure function $S(k)$ in units of the noise intensity $DN$ as a function of the wave number $2\pi k/N$ for $\tau=4$, $\varepsilon=-0.05$, $\sigma=10$, $K=0.1$, and different $\alpha$: $\alpha=0.4, 0.6, 1, 10$. Parameter $\alpha$ increases gradually from lower curve to the upper curve. Solid lines correspond to $S$ computed numerically for a ring of $N=2048$ coupled oscillators; dashed lines obtained from the analytic expression Eq. (10). Inset: solid lines show the wave number $2\pi k_{\max}/N$ at the maximum of $S$ as a function of $\alpha$. Dashed lines correspond to the minimum of $S$ with the smallest wave number $2\pi k_{\min}/N$. Thick lines indicate areas where $S(k_{\max})$ is larger than $S(0)$.

As time delay increases, $S/DN$ acquires a maximum at a certain nonzero wave number $2\pi k/N$. At $\tau=0$ there are no spatial correlations in the subthreshold fluctuations, as the homogeneous mode with $k=0$ has the largest energy. At $\tau=3$, the energy of the subthreshold fluctuations with the wave number at the peak of $S/DN$ is of the same order as the energy of the homogeneous mode. However, for $\tau=5$, the peak energy is larger than $S(k=0)/DN$, resulting in a well-pronounced spatial correlation on the length of $l_{\rm corr}=N/k_{\max}$, where $2\pi k_{\max}/N$ is the wave number at the peak.

To study the effect of the correlation length $1/\alpha$ of noise, we fix delay time to $\tau=4$ and compute $S(k)$ for different $\alpha$, both by numerical simulation of Eq. (1) and analytically, using Eq. (10). This is shown in Fig. 6. The upper curve in the main panel in Fig. 6 corresponds to almost uncorrelated noise, i.e., to $\alpha=10$. As $\alpha$ is decreased, two interesting phenomena occur. (i) First, the power of the noise-induced fluctuations at any finite wave number is decreased. This becomes clear as we gradually decrease $\alpha$ from $\alpha=10$ (upper curve) to $\alpha=1$, $\alpha=0.6$, and $\alpha=0.4$ given by the second, third, and fourth curves from the top, respectively. (ii) Second, the wave number $k_{\max}$ at the maximum of the structure function monotonically decreases with $\alpha$. At a certain value of $\alpha$, the power of the fluctuations at $k_{\max}$ equals the power of the homogeneous mode, i.e., $S(k_{\max})=S(0)$. For $\tau=4$, this situation corresponds to $\alpha=0.6$, which is given by the third curve from the top in the main panel in Fig. 6. On further decreasing $\alpha$, the maximum of $S(k)$ at a finite wave number $k_{\max}$ disappears, which means that external noise can no longer serve as an indicator of the spatial instability.

The inset in Fig. 6 shows how $k_{\max}$ changes with $\alpha$ for different delay times, as indicated by a number near each curve. On thick solid lines the power of the fluctuations at $k_{\max}$ is larger than the power of the homogeneous mode $S(0)$.

We now use Eq. (10) to find the range of the delay times $\tau$ for which the energy of the noise-induced fluctuations at finite wave number is larger than the energy of the homogeneous mode $k=0$. For uncorrelated noise ($\alpha=\infty$) and fixed

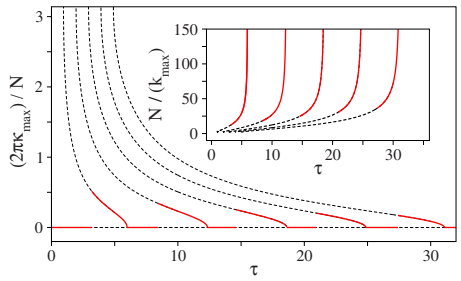


FIG. 7. (Color online) Wave number $2\pi k_{\max}/N$ at the maximum of the structure function vs delay time $\tau$ for $\alpha=\infty$, $\sigma=10$, and $K=0.1$. Solid lines indicate that the absolute value of the structure function $S(k=k_{\max})$ at the corresponding wave number is larger than $S(k=0)$. Inset shows spatial period $N/k_{\max}$ vs $\tau$.

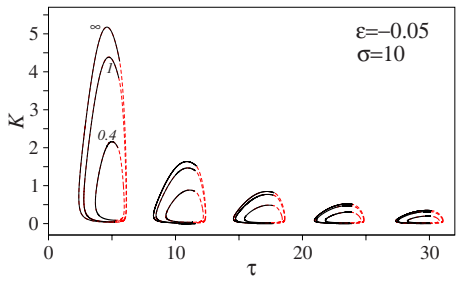


FIG. 8. (Color online) Areas on the $(\tau,K)$ plane, where $S(k_{\max})>S(0)$ for $\varepsilon=-0.05$ and $\sigma=10$. Numbers near each curve in the leftmost family indicate different values of $\alpha$. In the regions enclosed in the curves the structure function has a maximum at a finite nonzero wave number and this maximum is larger than $S(0)$. When crossing the solid lines: maximum appears (disappears) at a nonzero wave number. On the dashed lines wave number at the peak of the structure function becomes zero.

coupling strength $\sigma=10$ and $K=0.1$, we plot in Fig. 7 the wave number $2\pi k_{\max}/N$ at the peak as a function of the delay time. Solid lines highlight parameter values for which $S(0)<S(k_{\max})$.

Form Fig. 7 we see that for small $\tau$, the structure function acquires a maximum at zero wave number. However, there is a critical delay time around $\tau\approx 4$ when the maximum appears at the nonzero wavelength. As $\tau$ is increased, the wave number at the peak $2\pi k_{\max}/N$ decreases and at $\tau\approx 6$ it becomes zero again. This scenario repeats itself as $\tau$ is being increased further.

Figure 8 shows areas on the parameter plane $(\tau,K)$, where the structure function has a peak at a nonzero wave number, which is higher than $S(0)$. Three different values of $\alpha$, $\alpha=\infty$, $\alpha=1$, and $\alpha=0.4$, have been used as indicated by a number in the leftmost family of the closed curves. The order of curves, which correspond to different $\alpha$, is the same in each family; i.e., $\alpha$ increases from the inner to the outer closed curve.

The areas where $S(k_{\max})>S(0)$ are enclosed within the curves. On the solid lines the peak appears at a nonzero wave number; on the dashed lines the peak wave number becomes zero. Interestingly, time delay can no longer induce spatial correlations in the system if $K$ is increased above some critical value. For instance, for $\alpha=\infty$ and $\sigma=10$, this critical value is $K_c=5.16$.

## IV. CONCLUSION

To conclude, we considered a chain of deterministic and stochastic linear damped oscillators with time delay, coupled locally via a diffusive coupling. In the noiseless limit we studied the stability of the system with respect to spatiotemporal harmonic perturbations. For positive damping coefficient $\varepsilon$ and arbitrary but finite number $N$ of oscillators in the chain, time delay can stabilize the homogeneous steady state in the system. Depending on the coupling strength $\sigma$ and the feedback strength $K$, several islands of stability appear on the parameter plane $(\varepsilon,\tau)$ [see Figs. 1(b) and 1(c)]. We have shown that local time-delayed feedback induces multiplicity of neutral modes with different wave numbers and group velocities. Using analytical expression for the group velocity, we have demonstrated how the wave number and the velocity of the wave packet change with time delay.

In case of noisy oscillators we focused on the subthreshold regime. In this case, external noise serves as a precursor of spatial instability. We obtained an analytic expression for the structure function of subthreshold fluctuations induced by external noise correlated in space and uncorrelated in time. Using the analytic formulas for the structure function, we have shown that for finite correlation length of noise the wave number, which is excited with the largest energy, decreases as compared with the wave number for uncorrelated noise. Moreover, there exists a critical value of the correlation length of noise at which the energy of the homogeneous mode $S(0)$ becomes larger than the energy of any other mode. This shows that for a fixed subcriticality, i.e., at fixed values of all parameters of noiseless system, there exists such a correlation length of noise, below which external fluctuations can no longer serve as a precursor of spatial instability.

## ACKNOWLEDGMENT

This work was supported by Engineering and Physical Sciences Research Council (U.K.) Grant No. EP/D055075/1.

[1] M. Heckl, J. Acoust. Soc. Am. **36**, 1335 (1964).
[2] L. Cremer and M. Heckl, *Körperschall* (Springer-Verlag, Berlin, 1967).
[3] D. J. Mead and E. G. Wilby, Shock Vib. Dig. **35**, 45 (1966).
[4] D. J. Mead, J. Sound Vib. **27**, 235 (1973).
[5] D. J. Mead, J. Sound Vib. **40**, 1 (1975).
[6] D. J. Mead, J. Sound Vib. **11**, 181 (1970).
[7] F. Romeo and G. Rega, Chaos, Solitons Fractals **27**, 606 (2006).
[8] L. Manevitch, Nonlinear Dyn. **25**, 95 (2001).

[9] G. Chakraborty and A. Mallik, Int. J. Non-Linear Mech. **36**, 375 (2001).
[10] D. J. Mead, J. Sound Vib. **14**, 525 (1971).
[11] D. J. Mead, J. Sound Vib. **47**, 457 (1976).
[12] S. Boccaletti, D. Maza, H. Mancini, R. Genesio, and F. T. Arecchi, Phys. Rev. Lett. **79**, 5246 (1997).
[13] M. Bestehorn, E. V. Grigorieva, and S. A. Kaschenko, Phys. Rev. E **70**, 026202 (2004).
[14] L. Yang, M. Dolnik, A. M. Zhabotinsky, and I. R. Epstein, Phys. Rev. E **62**, 6414 (2000).
[15] W. Lu, D. Yu, and R. G. Harrison, Phys. Rev. Lett. **76**, 3316 (1996).
[16] M. Bertram and A. S. Mikhailov, Phys. Rev. E **63**, 066102 (2001).
[17] T. Pierre, G. Bonhomme, and A. Atipo, Phys. Rev. Lett. **76**, 2290 (1996).
[18] H. X. Hu, Q. S. Li, and L. Ji, Phys. Chem. Chem. Phys. **10**, 438 (2008).
[19] A. Neiman, P. I. Saparin, and L. Stone, Phys. Rev. E **56**, 270 (1997).
[20] J. Garcia-Ojalvo and J. M. Sancho, *Noise in Spatially Extended Systems* (Springer-Verlag, New York, 1999).
[21] J. Wu, *Introduction to Neural Dynamics and Signal Transmission Delay* (Walter de Gruyter, Berlin, 2001).
[22] H. Haken, Eur. Phys. J. B **18**, 545 (2000).
[23] H. Haken, Biosystems **63**, 15 (2001).
[24] J. Cao and J. Lu, Chaos **16**, 013133 (2006).
[25] S. Xu, J. Lam, D. W. C. Ho, and Y. Zou, J. Comput. Appl. Math. **183**, 16 (2005).
[26] J. Qiu and J. Cao, J. Franklin Inst. **346**, 301 (2009).
[27] C. M. González, C. Masoller, M. C. Torrent, and J. García-Ojalvo, Europhys. Lett. **79**, 64003 (2007).
[28] A. Pototsky and N. B. Janson, Phys. Rev. E **76**, 056208 (2007).
[29] V. Flunkert and E. Schöll, Phys. Rev. E **76**, 066202 (2007).